

## **Fabrication of Pomegranate Peel loaded nanofibers for adsorption of dyes in waste water samples**

Eashver Elango <sup>1</sup>, Subramanian Sundarrajan,<sup>2</sup> Guo Weijia<sup>2</sup> and Seeram Ramakrishna<sup>2,\*</sup>

<sup>1</sup>Affiliation 1; Student: eashvere@gmail.com

<sup>2</sup> Affiliation 2; Researcher: [sundar@nus.edu.sg](mailto:sundar@nus.edu.sg)

<sup>2</sup> Center for Nanofibers and Nanotechnology, Department of Mechanical Engineering, Faculty of Engineering, National University of Singapore, Singapore

\*Correspondence: [sundar@nus.edu.sg](mailto:sundar@nus.edu.sg) (S.S.); [seeram@nus.edu.sg](mailto:seeram@nus.edu.sg) (S.R.)

### **INTRODUCTION**

Textile industry has been a key pillar for many countries and dyeing is most widely used for coloration of fiber (Velmurugan et al,2011). The increased demand for textile products and their production lead to a proportional water consumption and massive wastewater discharge (Chequer et al, 2013). However, blatant dumping of colored dyes and effluents, especially some synthetic dyes, which is not easily biodegradable, can be toxic and have adverse effect on all forms of life. Nevertheless, even natural dyes are rarely non-harmful, due to some certain substances, such as chromium, that must be included to fix color on two the fabric (Kant et al,2017; Abbas et al, 2017). The discharged natural and synthetic dyes become the major source of the water pollution and affect human beings directly and indirectly. To remove the harmful substances and chemicals, including aniline, dioxin, formaldehyde and heavy metals such as zinc etc., various treatment methods for wastewater before discharge have been investigated [Amin et al,2009]. Currently, the separation technologies utilized in the dye removal of effluents includes filtration, membrane separation, adsorption, ion exchange, coagulation- flocculation and biological treatment (Kasperchik et al,2012; Mahmoodi et al, 2005; Rao et al, 2001; Salem et al, 2000; Jadhav et al, 2011; Makertihartha et al, 2017).

Over the past few years, oxidation, absorption and biological treatments are the most frequently studied and they have different advantages. Generally, adsorption has a high treatment efficiency and the adsorbents can be recycled, which is economically friendly. Also, in terms of its easy operation, simple design and insensitivity, adsorption is more popular than the other frequently used methods (Chuah et al, 2005). For the present study, the cost of the activated carbon commonly used is high and may regenerate carbon (Chuah et al, 2005; Ahmad et al, 2015). Indeed, newer technique or absorbent must bring about improvement to meet the increasingly stringent environmental limits and regulations.

Nanofibers have shown promising results as an absorbent due to its large surface-to-volume ratio. The process of electrospinning has allowed previous studies to create large volumes of nanofibers in a relatively low-cost way. Finally, the simplicity of the nanofibers membrane technique allows for large scale usage (Ramakrishna et al, 2006; Nasreen et al, 2019; Kaur et al, 2014; Sundarrajan et al, 2013; Kaur et al,2012a; Kaur et al 2012b). The subsequent nano fiber membranes made using phase inversion and drop-casting can also serve as an upcoming alternative to the active carbon

due to its increased surface area for better absorption. In tandem with agricultural waste, these are possible to serve as better dye filters than current solutions.

Conventionally, synthetic polymers have been employed as nanofibrous membranes (except few reports) in presence of functional materials to remove dyes and in the absence of functional materials, they are not effective for removing dyes. Also, widely used activated carbon has few drawbacks as it is mentioned above. In order to remove dyes, functional materials are introduced into nanofibers, which increases the cost. Therefore, an effective solution to these two issues requires addressing the limitations at these two concerns simultaneously. In order to overcome this problem, researchers have explored and innovated various sustainable materials into nanofibers. Natural polymers such as cellulose acetate, gelatin, and so on and natural material additives such as bitter melon, watermelon (Ramakrishna et al, 2006; Palaniswamy et al, 2018) and so on have been explored as sustainable materials to filter various pollutants in water. This can co-tackle the twin concerns of resource depletion and waste accumulation.

Recycled fruit peels have been used as the active filter ingredient in previous studies. The exploration of recycling fruit peels waste for the treatment of dye removal in water can be termed “waste-for-waste” approach. These fruit peels received significant attention due to their low-cost, antibacterial property, multifunctionality and environmental friendliness. Some of the studied materials are powder of avocado, dragon fruit, snow melon, watermelon, sweet lime, papaya, radish, bitter melon, and corn. Individually these fruit peels have been used to remove both heavy metals and textile dyes from wastewater (Ramakrishna et al, 2006; Palaniswamy et al, 2018). However, in comparison to those peels, pomegranate peels have performed better in terms of absorption. Pomegranate is a widely grown fruit crop, especially in tropical and subtropical regions. Its price is low, and its powder has shown promising performance to removal of different dyes from textile wastewater (Dehvari et al, 2015). The absorption of these fruit peels can be attribute to their surface functional groups. For example, the -COOH and -OH groups on avocado, dragon fruit, and snow melon peels allowed for the water purification. An analysis of the functional groups on the surface of a pomegranate peel may provide insight into its purification power (Palaniswamy et al, 2018).

Recycled fruit peels and cellulose acetate (CA) nanofibers are also sustainable materials. Dried pomegranate rind, due to its agricultural roots, is already biodegradable and CA, a derivative of a natural polymer, has been shown to be biodegradable and nontoxic (Alexander et al, 1993; Dhanush et al, 2019). Both can be discarded after adsorption without the need for material disposal. CA nanofibers have been utilized in human implants and other biological scaffolding applications and have shown minimal toxicity to biological organisms (Tsiapla et al, 2018).

In this study, the feasibility of using pomegranate as a dye filter is proved. The pomegranate powder is applied separately and subsequently mixed with polymers and then subjected to electrospinning. The absorptive capacity of electrospun nano fibers, pure pomegranate powder and polymer mixture were measured and compared by UV spectrophotometry system. The pure

pomegranate shows a decreased absorbance intensity. Fourier-transform infrared spectroscopy and contact angle measurement results were analyzed. Scanning electron microscopy (SEM) were also did to characterize the surface morphology. Some preliminary results are given in the presented study and provide the possibility of using pomegranate in the removal of methyl blue dye from wastewater.

## **MATERIALS AND METHODS**

The methyl blue dye was purchased from Sigma-Aldrich and used as received. Cellulose acetate (CA), dimethylformamide (DMF) and acetone were purchased from Sigma-Aldrich and used as received. The dye was diluted with DI water to prepare stock dye solution with a concentration of 50 mg/L. Pomegranates, bought from a supermarket, were peeled for the skin. The skin was washed with DI water and dried. The grinded powder was sieved to remove particles size over 1.2mm. The pomegranate powder was kept for absorption study as absorbents. 5.6g CA, 16g DMF and 24g of acetone were mixed as the polymer solution and stirred using magnetic stirrers. Pomegranates were bought from a store, peeled for their rind, and grinded into a powder.

To prepare polymeric membranes, phase inversion technique is used in our study. Two PIM membranes were created. PIM1 and PIM2 are prepared with 10.0g polymer solution and 0.05g, 0.15g pomegranate powder, respectively. The mixtures were cast on glass plate and then submerged in coagulation bath containing ice water. [Kaur et al, 2012b] The precipitation will take place for several minutes. The collected membranes were washed with de-ionized water and then dried in an oven for 2h, at 50°C.

Electrospinning technique was employed to produce the nano-scale fibers in this study. A typical procedure adopted for the preparation of a ENM01 is provided here. A syringe equipped with a needle of tip diameter 15 cm, 0.6 mm needle dia, provide a constant flow of 0.4 ml/h. The solution was then loaded into a syringe fitted to a pump. The positive terminal of a high voltage DC power supply (5KV) was connected to the metallic needle of the syringe. Electrospinning was carried out at room temperature in air with a relative humidity of 60%. The fibers were collected onto a rotating drum wrapped with non-stick aluminum foil for 6 hours and 45 minutes. This membrane hereafter referred to as ENM01. Similarly, nanofibers were also produced with the following conditions such as 0.8mm needle diameter, 0.4ml/hr, 10KV, 15 cm and 0.6 mm, 6cm, 0.4 ml/hour, 10KV conditions and they are hereafter referred to as ENM02 and ENM03, respectively. 20mg of the ENM03 nanofibers were drop-casted with 2ml of ethanol with 50mg of peel powder. To improve the structural integrity of the nanofibers, they were dried in an oven for 2h, at 50°C.

Scanning electron microscopy (SEM) images were obtained from a HITACHI S-4300. The phase inversion membranes or nanofiber samples were coated with gold prior to measure the SEM images. Fiber diameters were measured using Java image processing software [Image J 1.29(222 commands)].

30mg of pure pomegranate was mixed into 25ml stock solution (M1), while 1mg and 3mg of pomegranate powder in membrane (referred to as PIM1 and PIM2, respectively) were poured into

the 25ml dye solution respectively (referred to as M2 and M3). About 2mg of nanofibers produced from the electrospinning was used with the 25ml dye solution as well (M4).

The surface contact angles were measured using a Video Contact Angle System (VCA Optima, AST) equipped with an image processing and measuring tool. A micro needle on the apparatus dropped deionized water on to the phase inversion membranes and nanofiber samples below. A picture with the needle and drop was taken. Each sample had three separate drops and thus three pictures. These drops were averaged to produce the average contact angles.

### 3. RESULTS

#### Characterization of the nanofibers

##### Surface morphology by SEM

To study the surface morphology and fundamental physical properties of the nanofibers prepared from electrospinning, the scanning electron microscope (SEM) was taken as the primary tool. Figure 1 shows the SEM image of the ENM 01 nanofibers. When the operating voltage was set at 5 KV (Figure 1a and 1b), nanofibers formed were of honeycomb structures as it is rarely reported in literature (Greiner et al, 2007) and does not form smooth and uniform fibers. It is already reported by us and others that by increasing the voltage, it is possible to tune the nanofibers diameter and morphology (Greiner et al,2007; Ramakrishnan et al, 2007). Further study was carried out in order to find out whether increasing the voltage will tend to form nanofiber with cylindrical morphology. In the next experiment, the voltage was increased to 10KV and the SEM image of nanofibers formed is shown in Figure 1c and 1d. Apart from the formation of smooth nanofibers, formation of few beaded fibers morphology were also observed. Figure 2 show the SEM image of the ENM 03 nanofibers of having diameter between 80-250nm. However, beads were observed for nanofibers with relatively larger diameters. The enlarged SEM shows that the nanofibers can be free of beads, which means that straight nanofibers with smaller diameter can be produced (Figure 2).

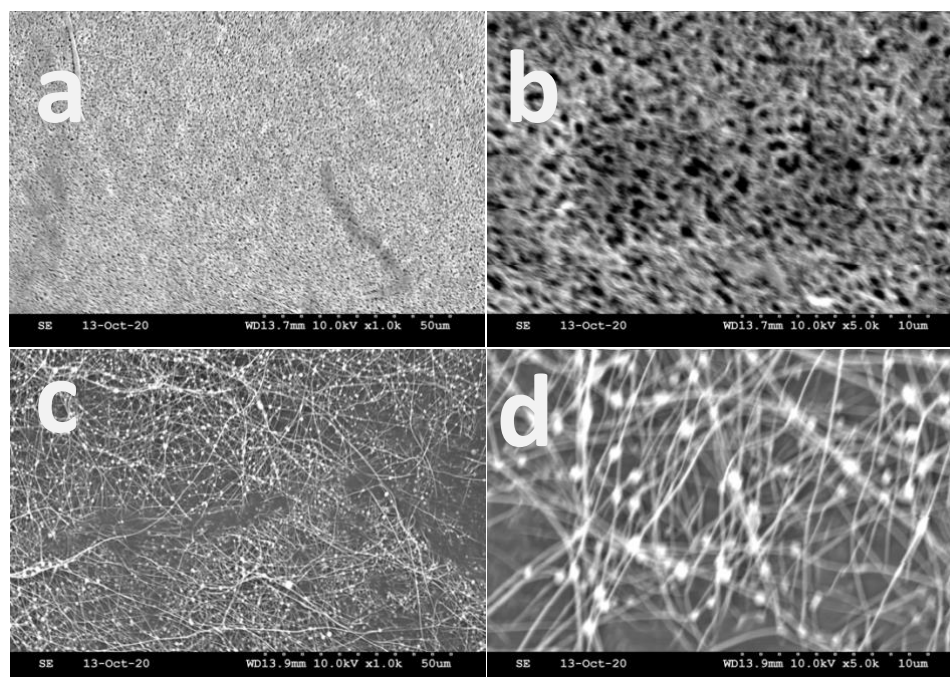


**Figure 1.** SEM image of the nanofiber produced from electrospinning at varying electrospinning conditions, (a) 0.6 mm, 15 cm, 0.4 ml/hour, 5KV, Image of nanofibers at 1000X magnification (b) same nanofiber image at 5000x magnification; 0.8 mm, 15 cm, 0.4 ml/hour, 10KV (c) Image of nanofibers at 1000X magnification, and (d) at 5000x magnification.

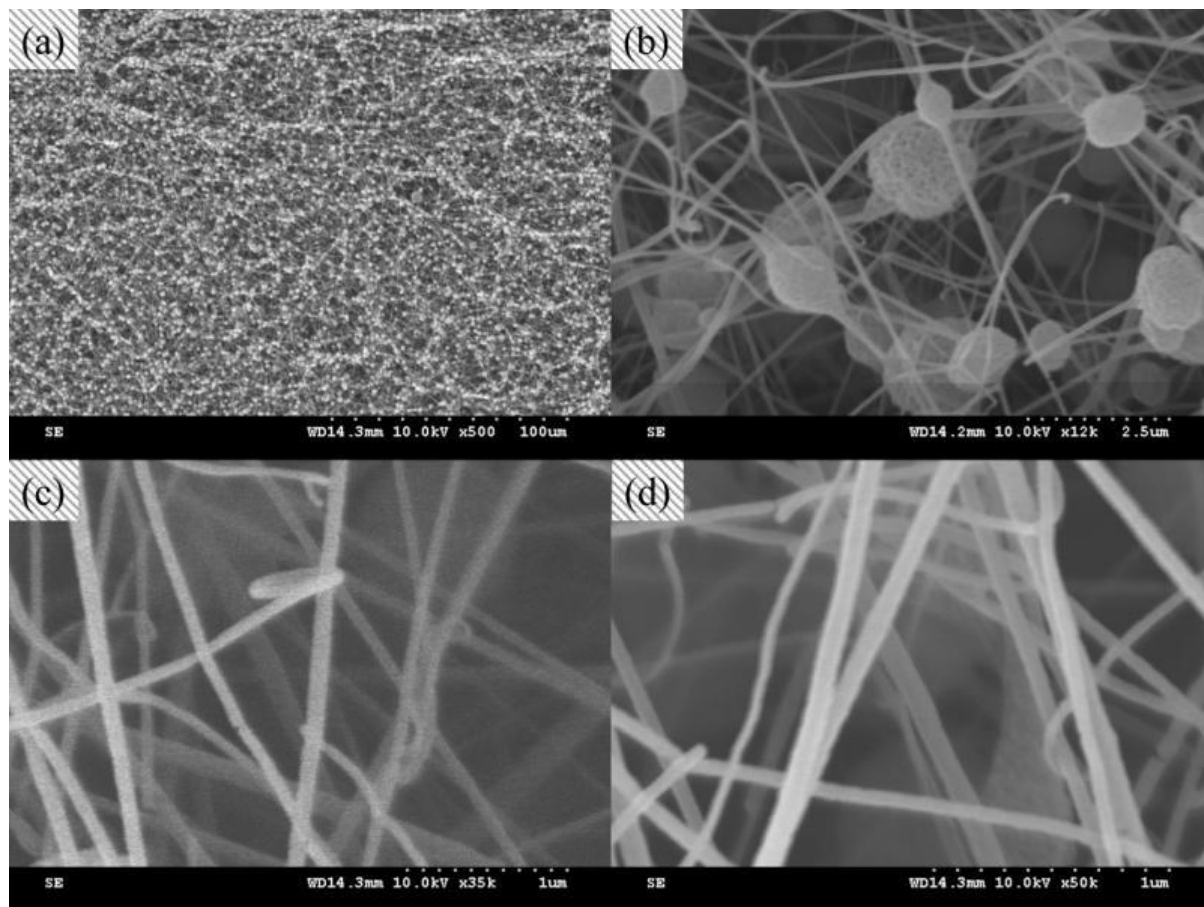


**Figure 2.** Scanning electron micrograph of the nanofiber produced from electrospinning (0.4ml/hr,10KV,15 cm) at varying magnifications (a) Image of nanofibers at 500X magnification (b) Image of nanofibers at 12000x magnification (c) Image of nanofibers at 35000x magnification (d) Image of nanofibers at 50000x magnification

The SEM images of PIMs are displayed in Figure 3. It has been observed that there is a gradual increase of pore size from PIM 0 to PIM 1 and PIM2, which could be due to blending of pomegranate powder with cellulose acetate, whereby phase separation occurs between hydrophilic CA and hydrophobic pomegranate powder when the cast polymer film is kept in the coagulation bath (water).

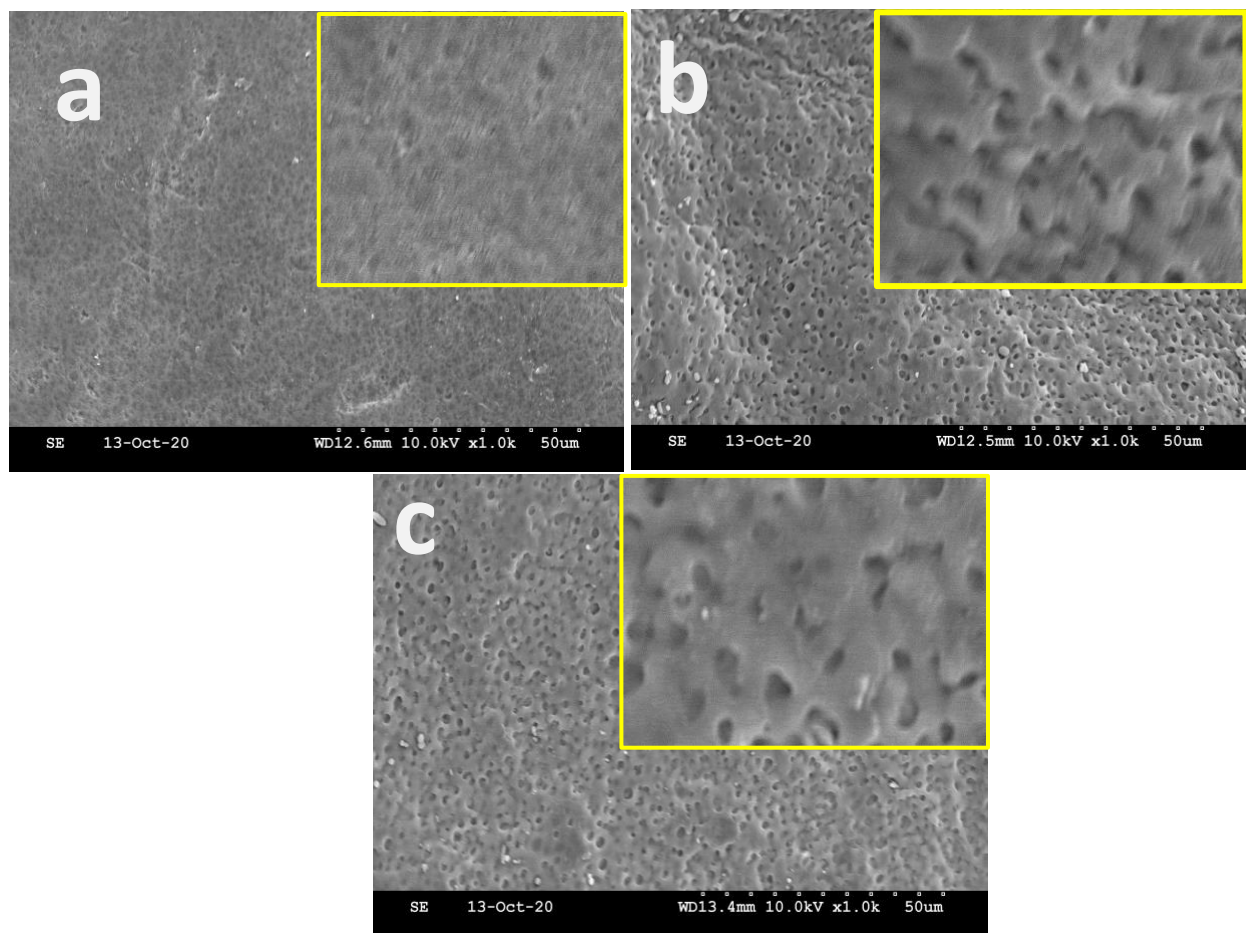


**Figure 3.** SEM of phase inverted membranes: (a) CA without pomegranate powder, (b) CA with pomegranate powder (PIM1), and (c) CA with pomegranate powder (PIM2) (insets images are magnified by 4 times of their corresponding images).

### FTIR spectrum analysis

The FTIR spectra range from  $4000\text{ cm}^{-1}$  to  $400\text{ cm}^{-1}$  of the nanofibers are shown as in Figure 4. The strong peak at  $1740\text{ cm}^{-1}$  can be attributed to C=O carboxyl group, showing the potential for carboxylic acids, ketones and aldehydes (Smith et al, 2018). The  $1368\text{ cm}^{-1}$  band is related to  $\text{CH}_2$ , which shows the appearance of cellulose, validating the FTIR peaks (Li et al, 2009). The other two strong peaks are at  $1232\text{ cm}^{-1}$  and  $1046\text{ cm}^{-1}$ , both confirm the existence of ester functional groups (Sheu et al, 1989).

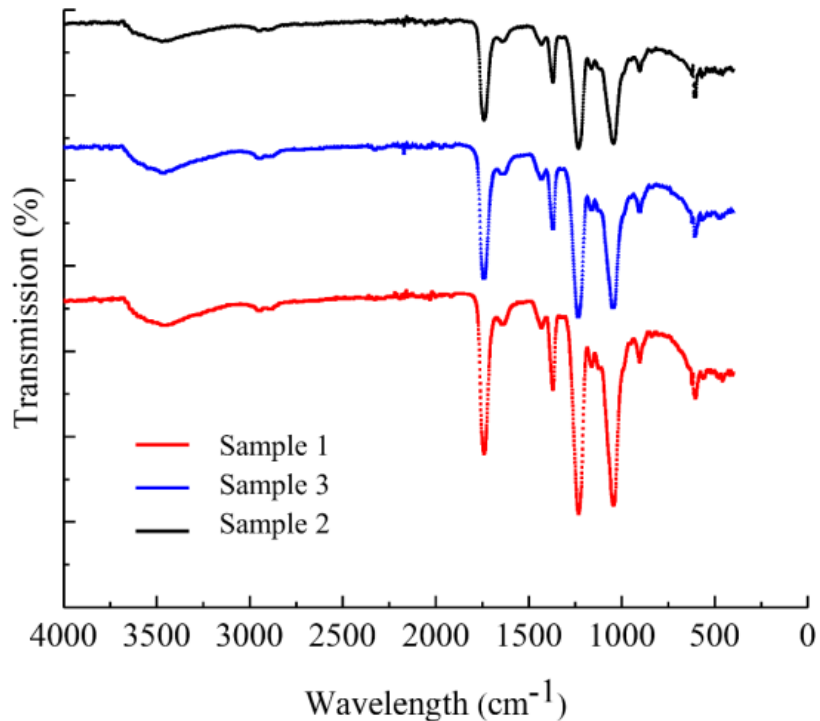


**Figure 4.** FTIR transmission spectra of the nanofibers created with 10kV voltage at 15 cm of distance with a flow rate of 0.4 ml/hour. Sample 1 comprises of cellulose created with 6mm needle while Sample 2 and Sample 3 are created with pomegranate powder with 8mm needle

### UV-visible study

UV-visible study was carried out for the mixture M1, M2, M3 and M4, as given in 2.4 to compare the absorbance value after different duration of dye absorption. Figure 5 shows the pomegranate powder filtered out of methyl blue dye solution after its UV absorbance test. The color of the pomegranate powder (M1) turned to green and discoloring the test water. This change in colour indicates that the dyes are adsorbed onto the pomegranate powder.

In the cases of M2, M3 and M4 samples, they all showed a different trend when compared with M1. For the phase-inversion membrane (M2), the absorbance trended downward, yet acted very slowly. After 15 hours, which is not shown in Figure 6, the absorbance can reach to a low value of 0.1276. The membrane maintained the blue colour of the dye, showing that the dye is indeed absorbed and retained in the structure. For the mixture M4, the membrane has 3 times amount of pomegranate powder included, compared to PIM1 (M2). After 15 hours, the absorption value can also be reduced to 0.1055. However, the visual colour looked darker than that of M2, which create a visual cue to the increased absorption that the membrane provided.

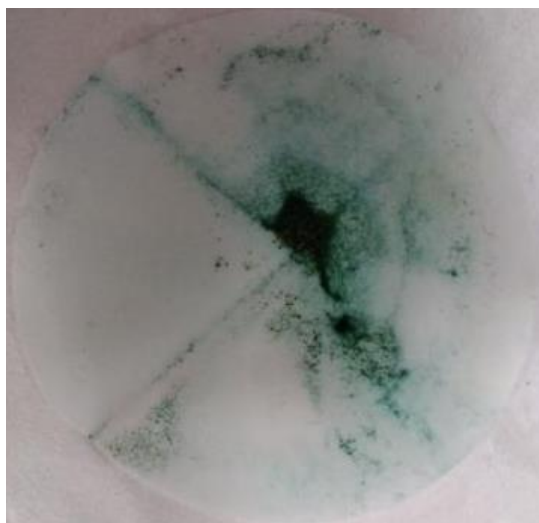


**Figure 5.** Pomegranate sediment after 1 hour of dye absorption

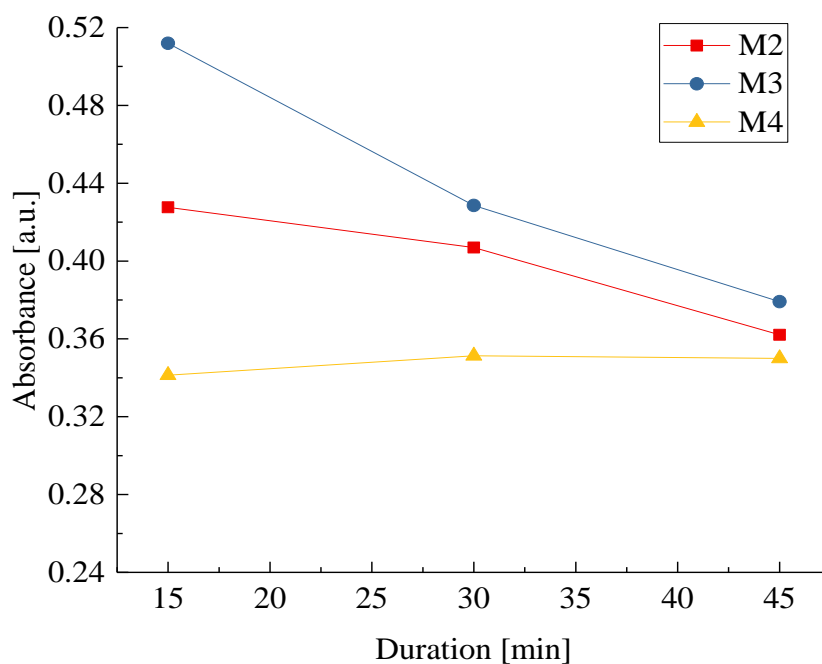


**Figure 6.** Change in absorbance with time for solutions of M2, M3, and M4

### Contact angle measurements

The static contact angle measurements in this study were measured through drop observation. Figure 7 shows examples of droplets on each of the three samples. Figure 7a represents a water droplet on a sample of nanofiber without of having any pomegranate powder. The contact angle of this CA nanofiber was measured as  $62.74^\circ$  showing the low hydrophobicity of the nanofibers to water. Coating of pomegranate powder on the nanofiber surface has increased the

hydrophobicity of the CA nanofiber. This had a contact angle value of  $87.39^\circ$  showing higher hydrophobicity (Figure 7b) than CA with water. However, with a very similar creation, by increasing the concentration of pomegranate (0.15 g to coat) , as shown in Figure 7c. has an even higher hydrophobicity with a measured contact angle of  $125.636^\circ$ . This could possibly due to the hydrophobic group contribution from the pomegranate powder.

The contact angles of the phase inversion membranes CA, PIM1, and PIM2 were measured and found to be  $0^\circ$  for all these membranes. The water drop, upon contact with these membranes, was suddenly absorbed and disappeared (contact angle analysis figure is not presented here). It is to be noted that CA has a contact angle of  $63.4^\circ$  in film form. This change of hydrophilic nature for the phase inverted membranes is due to the presence of hydrophilic functional groups on the surface during phase inversion process.

When we compare SEM images of ENMs (ENM1 to ENM3) (Figures 1 and 2) with PIM1 and PIM2 (Figure 3), the porosity of ENMs is larger than PIMs. Hence, ENMs contain a larger amount of air when compared to PIM 1 and PIM2. Also, inherent roughness of the ENMs are higher, which also provides to the observed higher CA, which is already reported by many authors (Kaur et al, 2012b)

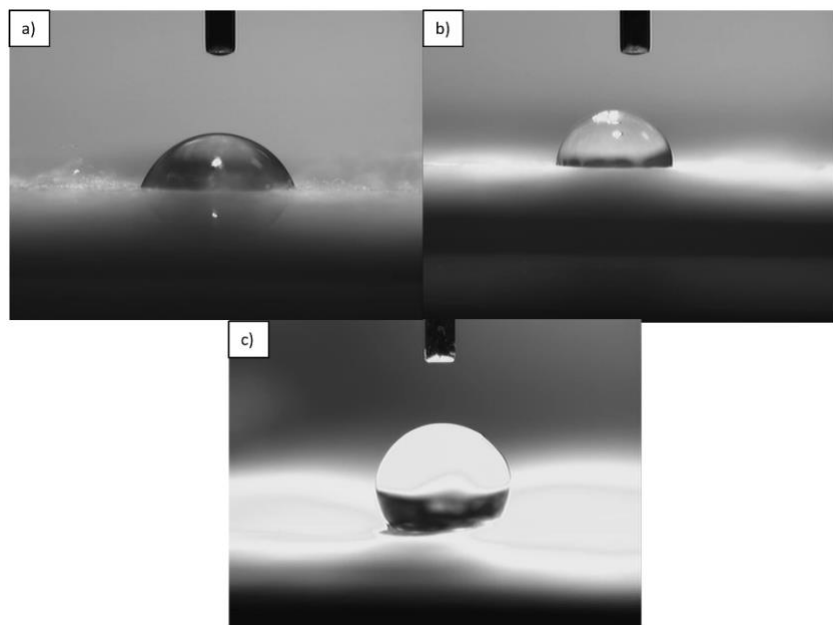


**Figure 7.** Contact Angle Pictures of three water droplets on nanofibers with a) Pure cellulose membrane sample b) 0.005g/L pomegranate powder membrane sample c) 0.015g/L pomegranate powder membrane sample.

## CONCLUSIONS

Based on our observation, pure pomegranate powder had the ability to adsorb the methyl blue dye and discolored the water. The phase-inversion membranes allowed for increased absorption at the cost of increased material required. The combination of polymer with pomegranate allowed for greater absorption compared to pure pomegranate powder. Even in the phase-inversion membranes, increasing the concentration of pomegranate powder had a measurable impact on the absorption of the membrane. The nanofibers were the most efficient in terms of absorption for mass of membrane. This study shows that the proposed nanofibers with pomegranate rind can be used as a sustainable material for the efficient degradation of dyes in the wastewater treatment.

**Funding:** This research received no external funding

## REFERENCES

- Abbas L.M., Hamdy Y.M. 2017 Synthesis and Characterization of Magnetic Nanoparticles with Plant Water Extract and their Application for Water Treatment. *Der Pharma Chem.* **9(24)**, 38-42.
- Ahmad, A., Mohd-Setapar, S.H., Chuong, C.S., Khatoon, A., Wani, W.A., Kumar, R., Rafatullah M. 2015 Recent advances in new generation dye removal technologies: novel search for approaches to reprocess wastewater. *RSC Advances* **5(39)**, 30801-30818.
- Amin, N.K. 2009 Removal of direct blue-106 dye from aqueous solution using new activated carbons developed from pomegranate peel: adsorption equilibrium and kinetics. *Journal of Hazardous Materials* **165** (1-3), 52-62.
- Alexander Ach, 1993 Biodegradable Plastics Based on Cellulose Acetate. *Journal of Macromolecular Science partA.* **30 (9-10)**, 733-740.
- Chequer, F.M.D., Oliveira, G.A.R., Ferraz, E.R.A., Cardoso, J.C., Zanoni, M.V.B., Oliveira D.P. Textile Dyes: Dyeing Process and Environmental Impact. 2013 In *Eco-Friendly Textile Dyeing and Finishing*; Günay, M; IntechOpen,. DOI: 10.5772/53659.
- Chuah, T.G., Jumasiah, A., Azni, I., Katayon, S., Thomas Choong, S.Y. 2005 Rice husk as a potentially low-cost biosorbent for heavy metal and dye removal: an overview. *Desalination* **175**, 305–316.
- Dhanush G., Sundarrajan,S., Seeram R., Bio-based Nanofibers involved in wastewater treatment, **2019** *Macromolecular Materials and Engineering* 1900345,
- Dehvari, M., Ghaneian, M.T., Ebrahimi, A., Jamshidi, B., Mootab, M. 2015 Removal of reactive blue 19 dyes from textile wastewater by pomegranate seed powder: Isotherm and kinetic studies. *International Journal of Environmental Health Engineering* **5** (1, 5).
- Greiner, A., Wendorff, J.H. **2007** Electrospinning: A Fascinating Method for the Preparation of Ultrathin Fibers, *Angewandte Chemie International English Edition* **46**, 5670-5703.
- Jadhav, S.B., Swapnil S.P., Pratibha S.P., Jyoti P.J. **2011** Biochemical degradation pathway of textile dye Remazol red and subsequent toxicological evaluation by cytotoxicity, genotoxicity and oxidative stress studies. *International Biodeterioration & Biodegradation* **65 (6)**, 733-743.
- Kant, R. **2012** Textile dyeing industry an environmental hazard. *Journal of Nature and Science* **4 (22-26)**. doi: 10.4236/ns.2012.41004.
- Kasperchik, V. P., Yaskevich, A.L., Bil'Dyukevich, A.V. **2012** Wastewater treatment for removal of dyes by coagulation and membrane processes. *Petroleum Chemistry* **52(7)**, 545-556.

- Kaur, S., Sundarrajan, S., Rana, D., Sridhar, R., Gopal, R., Matsuura, T., Ramakrishna, S. **2014** Review: the characterization of electrospun nanofibrous liquid filtration membranes. *Journal of Materials Science* **49**, 6143–615.
- Kaur, S., Sundarrajan, S., Matsuura, T., Ramakrishna, S. **2012a** Influence of electrospun fiber size on the separation efficiency of thin film nanofiltration composite membrane. *Journal of Membrane Science* **392-393**, 101-111.
- Kaur, S., Rana, D., Matsuura, T., Subramanian, S., Ramakrishna, S. **2012b** Preparation and Characterization of Surface Modified Electrospun Membranes for Higher Filtration Flux. *Journal of Membrane Science* **390-391**, 235-242.
- Li, Z., Jiang, W. **2009** Interlayer conformations of intercalated dodecyltrimethylammonium in rectorite as determined by FTIR, XRD, and TG analyses. *Clays Clay Minerals* **57(2)**, 194-204.
- Mahmoodi, N.M., Yousefi L.N., Salman T.N. **2005** Decolorization and Aromatic Ring Degradation Kinetics of Direct Red 80 by UV Oxidation in the Presence of Hydrogen Peroxide Utilizing TiO<sub>2</sub> as a Photocatalyst. *Chemical Engineering Journal* **112**, **191-196**. 10.1016/j.cej.2005.07.008.
- Makertihartha, I.G.B.N., Rizki Z., Zunita M., Dharmawijaya P.T. **2017** Dyes removal from textile wastewater using graphene based nanofiltration. *AIP Conference Proceedings* **1840** ( 1), p. 110006.
- Nasreen, S.A.A.N., Sundarrajan, S., Nizar, S.A.S., Ramakrishna, S. **2019** Nanomaterials: Solutions to Water-Concomitant Challenges. *Membranes*, **9**, 40.
- Palaniswamy, R. **2018** Bioadsorption of Dyes using Vegetable and Fruit Peels, *Research Journal of Chemical and Environmental Sciences* **6[3]**, 17-19.
- Ramakrishna, S., Fujihara, K., Teo, W., Yong, T., Ma, Z, Ramaseshan, R. **2006** Electrospun nanofibers: solving global issues. *Materials Today* **9**, 40-50.
- R. Ramakrishnan, S.Sundarrajan, J. Rajen, S. Ramakrishna, **2007** Nanostructured Ceramics by Electrospinning, *Journal of Applied Physics* **102**, 111101.
- Rao N.N., Somasekhar K.M., Kaul S.N., Szyrkowicz L. **2001** Electrochemical oxidation of tannery wastewater. *Journal of Chemical Technology & Biotechnology* **76**, 1124–1131. doi:10.1002/jctb.493
- Salem, I., El-Maazawi, M. **2000** Kinetics and Mechanism of Color Removal of Methylene Blue with Hydrogen Peroxide Catalyzed by Some Supported Alumina Surfaces. *Chemosphere*, **41**, 1173-80. 10.1016/S0045-6535(00)00009-6.
- Sheu, L.L., Knozinger, H., Sachtler, W.M.H. **1989** Characterization by CO/FTIR spectroscopy of palladium supported on NaY zeolites. *Journal of Molecular Catalysis* **57**( 1), 61-79.
- Smith, B.C. **2018** The C=O bond, part III: Carboxylic acids. *Spectroscopy*, **33**. 14-20.
- Sundarrajan, S., Ramakrishna, S. **2013** New Directions in Nanofiltration Applications – Are Nanofibers the Right Materials as Membranes in Desalination?. *Desalination*, **308**, 198-208.
- Tsiapla, AR, Karagkiozaki, V, Bakola, V, et al. **2018** Biomimetic and biodegradable cellulose acetate scaffolds loaded with dexamethasone for bone implants. *Beilstein Journal of Nanotechnology* **9**, 1986-1994.
- Velmurugan, P.; Rathina, K. V; Dhinakaran, G. **2011** Dye removal from aqueous using low cost adsorbent. *International Journal of Environmental Science*. **1**, 7.

## Figure Captions

**Figure 1.** SEM image of the nanofiber produced from electrospinning at varying electrospinning conditions, (a) 0.6 mm, 15 cm, 0.4 ml/hour, 5KV, Image of nanofibers at 1000X magnification (b) same nanofiber image at 5000x magnification; 0.8 mm, 15 cm, 0.4 ml/hour, 10KV (c) Image of nanofibers at 1000X magnification, and (d) at 5000x magnification.

**Figure 2.** Scanning electron micrograph of the nanofiber produced from electrospinning (0.4ml/hr,10KV,15 cm) at varying magnifications (a) Image of nanofibers at 500X magnification (b) Image of nanofibers at 12000x magnification (c) Image of nanofibers at 35000x magnification (d) Image of nanofibers at 50000x magnification

**Figure 3.** SEM of phase inverted membranes: (a) CA without pomegranate powder, (b) CA with pomegranate powder (PIM1), and (c) CA with pomegranate powder (PIM2) (insets images are magnified by 4 times of their corresponding images).

**Figure 4.** FTIR transmission spectra of the nanofibers created with 10kV voltage at 15 cm of distance with a flow rate of 0.4 ml/hour. Sample 1 comprises of cellulose created with 6mm needle while Sample 2 and Sample 3 are created with pomegranate powder with 8mm needle

**Figure 5.** Pomegranate sediment after 1 hour of dye absorption

**Figure 6.** Change in absorbance with time for solutions of M2, M3, and M4

**Figure 7.** Contact Angle Pictures of three water droplets on nanofibers with a) Pure cellulose membrane sample b) 0.005g/L pomegranate powder membrane sample c) 0.015g/L pomegranate powder membrane sample.